radical anion (III$^{\ominus}$) has been noticed by previous workers [6]. This unsatisfactory feature seems thus to be shared not only by the radical anion of the 6-phenylderivative (II$^{\ominus}$), but also by that of the structurally related azuleno[5.6.7-*cd*]phenalene (I$^{\ominus}$).

It is tempting to use the HMO model of I for an estimation of the energy gap between the orbitals ψ_S and ψ_A. The diagram of Figure 6 suggests a value less than $0.1|\beta| \approx 0.25$ eV if the number k is not decreased below 0.75. Such a small energy gap might result in a triplet ground state of the dianion I$^{2\ominus}$. However, although this dianion is readily formed, its glassy solution in MTHF fails to display ESR. signals characteristic of the triplet state (*cf.* Experimental Part). It must therefore be concluded that I$^{2\ominus}$ has a singlet ground state and that more sophisticated MO methods are required to rationalize this finding in terms of orbital energies.

REFERENCES

[1] *F. Gerson*, «Hochauflösende ESR.-Spektroskopie dargestellt anhand aromatischer Radikal-Ionen», Verlag-Chemie, Weinheim, 1967; English Edition: 'High Resolution ESR Spectroscopy', Verlag-Chemie, Weinheim, and J. Wiley & Sons, New York, 1970.

[2] *Ch. Jutz, R. Kirchlechner & H.-J. Seidel*, Chem. Ber. *102*, 2301 (1969).

[3] *E. D. Bergmann & R. Ikan*, J. Amer. chem. Soc. *78*, 482 (1955); *H. Pommer*, Archiv. Pharm. *291/63*, 23 (1958); *Ch. Jutz et al.*, Chem. Ber., in press.

[4] *H. Fischer & G. Ege*, Chem. Ber. *100*, 395 (1967).

[5] *E. Heilbronner*, in 'Non-Benzenoid Aromatic Compounds' (D. Ginsburg, ed.). J. Wiley & Sons (Interscience), New York, 1959; pp. 171–276.

[6] *I. Bernal, P. H. Rieger & G. K. Fraenkel*, J. chem. Physics *37*, 1489 (1962).

[7] *A. H. Reddoch*, J. chem. Physics *43*, 225 (1965).

[8] *F. Gerson, J. Heinzer & E. Vogel*, Helv. *53*, 95 (1970).

[9] *A. D. McLachlan*, Mol. Physics *3*, 233 (1960).

---

156. Comparison of ¹³C- and ¹H-Magnetic Resonance Spectroscopy as Techniques for the Quantitative Investigation of Dynamic Processes. The Cope Rearrangement in Bullvalene

by **Jean F. M. Oth, Klaus Müllen, Jean-Marie Gilles** and **Gerhard Schröder**

Laboratory for organic chemistry, E.T.H., CH–8006 Zürich
Institute for organic chemistry, University of Karlsruhe, D–7500 Karlsruhe

(15. V. 74)

Summary. The potential advantages of ¹³C-(¹H-noise decoupled) spectroscopy (in the *Fourier* transform mode) over ¹H-spectroscopy for the quantitative investigation of molecular dynamic processes is discussed. The *Cope* rearrangement in bullvalene, an example of complex exchange of spins over different magnetic sites, has been studied by both kinds of spectroscopy as a test.

1. Introduction. – Temperature dependent NMR. spectra of molecules undergoing fast dynamic processes can in principle be quantitatively analysed and the kinetic data characteristic of the dynamics thus be obtained. The required line shape

calculations are easily made when the nuclei in exchange are not coupled among themselves or with other nuclei on stable magnetic sites[1]). The formalism of *Gutowsky & Holm* [1] is then entirely satisfactory when the dynamic process interconverts two isodynamic[2]) (one rate parameter) or two non isodynamic (two rate parameters) structures. The stochastic approach of *Anderson* [2], *Kubo* [3] and *Sack* [4] can be very successfully used in the more complicated situations where more than two structures are implicated – all structures could be isodynamic or not – and when more than one process is responsible for the exchange.

If the exchanging nuclei are coupled among themselves or with other nuclei on stable sites[1]) – this is the general situation in proton magnetic resonance – an exact line shape calculation can seldom be made. When only two structures (isodynamic or not) are implied, the formalism of *Alexander* [5] (generalized by *Delpuech* [6] and later by *Binsch* [7]) can however be used in favourable cases. In more complex exchange processes (more than two structures or more than two rates implied) and when the exchanging nuclei are coupled, exact calculations of line shape are practically excluded. In some particularly favourable cases however some approximations can be introduced and the line shape calculated. When for instance the splitting patterns due to the exchanging nuclei are, in the slow exchange limit, of first order or nearly first order, a useful approximation consists in the introduction of pseudo sites[3]) in place of the true sites and of an adequate treatment of the problem with the stochastic formalism. This approach was used successfully for the quantitative evaluation of the ^{1}H-NMR. spectra of some annulenes [9].

The complications due to internuclear couplings as generally encountered in ^{1}H-NMR. spectra must in principle disappear in ^{13}C-(^{1}H-noise-decoupled) spectra. The ^{1}H-noise-decoupled ^{13}C-spectrum in absence of exchange consists of sharp lines, each one characterizing one magnetic site. However, the intensity of these lines is proportional to the nuclei population on the sites only if adequate conditions are used to accumulate the free induction decays, to eliminate the ^{1}H-^{13}C *Overhauser* effects and to compute the *Fourier* transform[4]). The carefully recorded ^{13}C temperature edpendent spectra of dynamic systems undergoing the most complicated exchange can thus be quantitatively evaluated without approximation and simulated correctly using the stochastic formalism. In fact, as we will see later, valuable information concerning complicated exchange processes can also rapidly be obtained from the initial broadening observed for some lines of the spectrum.

In order to evaluate the evident advantages that ^{13}C-spectroscopy potentially possesses over ^{1}H-spectroscopy for the investigation of complex dynamic processes, we have investigated the ^{1}H-noise-decoupled ^{13}C-spectra of tricyclo[3.3.3.0^{4,6}]deca-

---

[1]) By stable magnetic sites we mean such sites which are occupied permanently by the same nuclei, *i.e.* by nuclei not involved in the exchange.

[2]) The term 'isodynamic' was introduced by S. Altman, Proc. Roy. Soc., *A 298*, 184 (1967), to describe a process relating structures which are superposable. The term applies also to the structures themselves.

[3]) The pseudo-site approximation was introduced by J.-M. Gilles, Thèse de doctorat (Physique), Université Libre de Bruxelles, 1969.

[4]) For details concerning the influence of the different experimental parameters in FT-spectros copy, see T. C. Farrar and E. D. Becker, Pulse and Fourier Transform NMR., Academic Press, New York 1971.

triene (bullvalene) [10]. We have also reinvestigated the ^{1}H-spectra. The kinetic parameters obtained by both methods are compared and discussed.

2. Bullvalene. – 2.1 *Dynamic properties of bullvalene.* The dynamic properties of the bullvalene molecule were predicted by *Doering & Roth* [10]. They suggested that any of the three cyclopropane bonds could be involved in a *Cope* rearrangement,
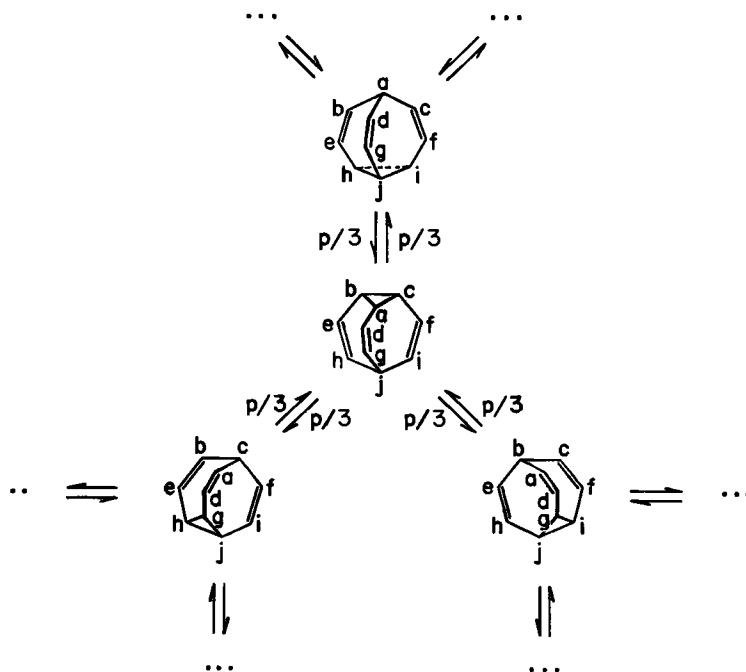

Fig. 1. *The three isomerization pathways in bullvalene*

the chemical identity of the molecule remaining unchanged during this process. Due to the three possible isomerization pathways that can be followed, any of the ten $\equiv$CH groups can occupy any position in the molecule in the course of time. This implies that no pair of C-atoms remains permanently linked together and also that for fast isomerization rates (with respect to the NMR. time scale) all $\equiv$CH groups must become magnetically equivalent and thus that the ^{1}H- and ^{13}C-(^{1}H-noise-decoupled) spectra must consist of one single line. This prediction of *Doering & Roth* was verified by us in 1963 when this molecule was first synthesized by *Schröder* [11]. Figures 2 and 3 reproduce some of the ^{1}H- (100 MHz) and of the ^{1}H-noise-decoupled ^{13}C-spectra (25 MHz) recorded for the purpose of this work and clearly illustrate the dynamic behaviour of the bullvalene molecule.

2.2 *Structure of the graph representing the interrelations between all the isomers implied by the* Cope *rearrangement.* Any permutation of the $\equiv$CH groups is feasible by a suitable sequence of elementary isomerizations. The total number of isomers implied by the dynamic process is thus 10!/3 (1.209.600), *i.e.* eon third of the total number

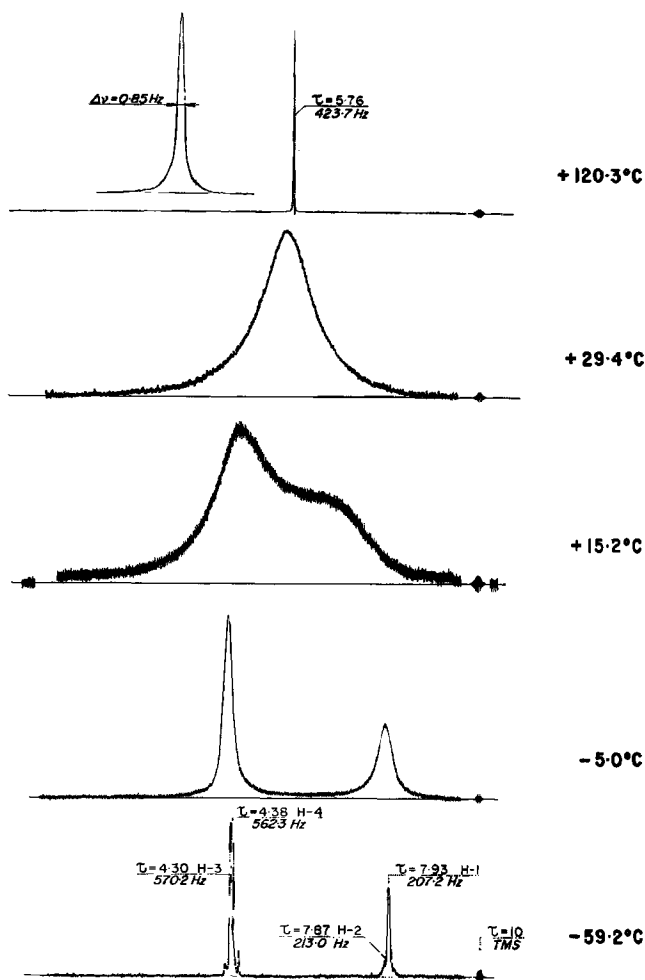Fig. 2. *¹H-NMR.-spectra of bullvalene in CS_2 recorded at different temperatures* (100 MHz, TMS as internal reference)

of permutations of 10 objects (the factor 1/3 results from the fact that the molecule has a C_3 symmetry axis, thus making indistinguishable three labelled[5]) isomers related one to the other by the symmetry operations C_3 and C_3^2).

It seemed to us interesting to investigate the structure of the graph representing the interrelations between these 10!/3 isomers. The graph considered here consists of 10!/3 points, each one representing a structure with the ≡CH groups labelled[5]).

[5] By labelled structure we mean a structure in which the different nuclei (or groups) are labelled (by letters). A label is permanently attached to a given nucleus. This allows to follow the change in chemical site that this nucleus undergoes in the course of the dynamic process.

[6] For the definition of a cycle in graph theory, see C. Berge, Graphes et Hypergraphes, Chapter 2, Dunod, Paris, 1970.
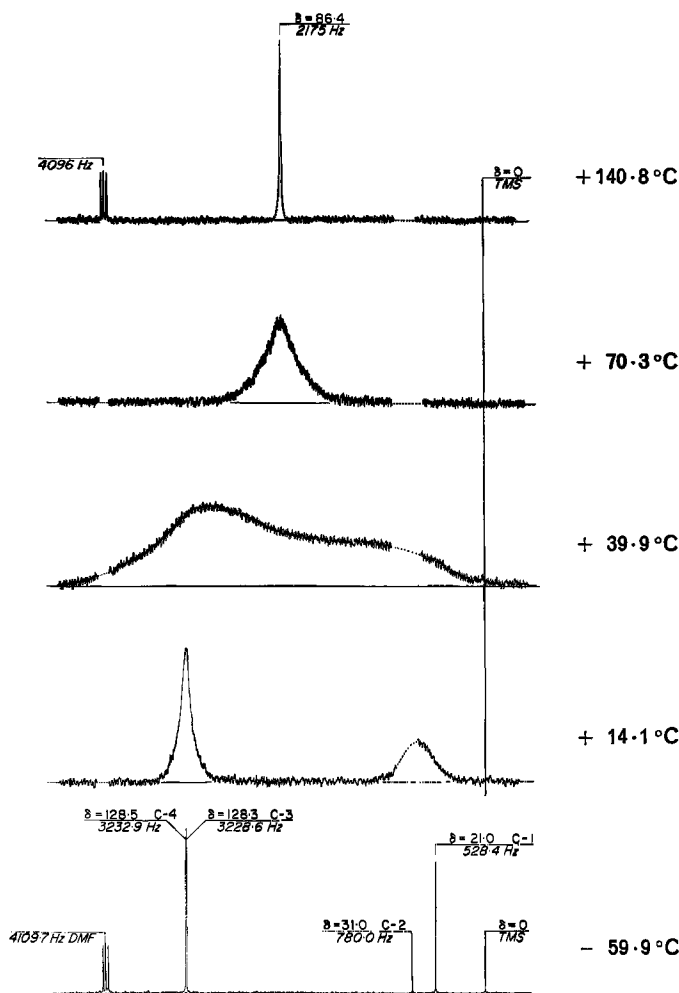
Fig. 3. *13C-NMR.-spectra of bullvalene in DMF-d7 obtained at different temperatures* (25 MHz, FT mode, 1H-noise-decoupled, the signals of TMS or of the carbonyl C of the solvent were used as internal reference). For clarity, the methyl signals of the solvent are not represented.

Each point is connected by three arcs to three other points, one arc representing one specific reversible elementary isomerization step. It can be shown that the graph so defined possesses the following characteristics:

– The shortest ('elementary' in the terminology used in graph theory) cycle[6]) of the graph counts 14 points. Such a cycle corresponds to a sequence of 14 labelled structures as represented in Figure 4;

– Each point of the graph is common to three such cycles;

– Each arc is common to two different cycles;

– The graph is most likely non planar[7]).

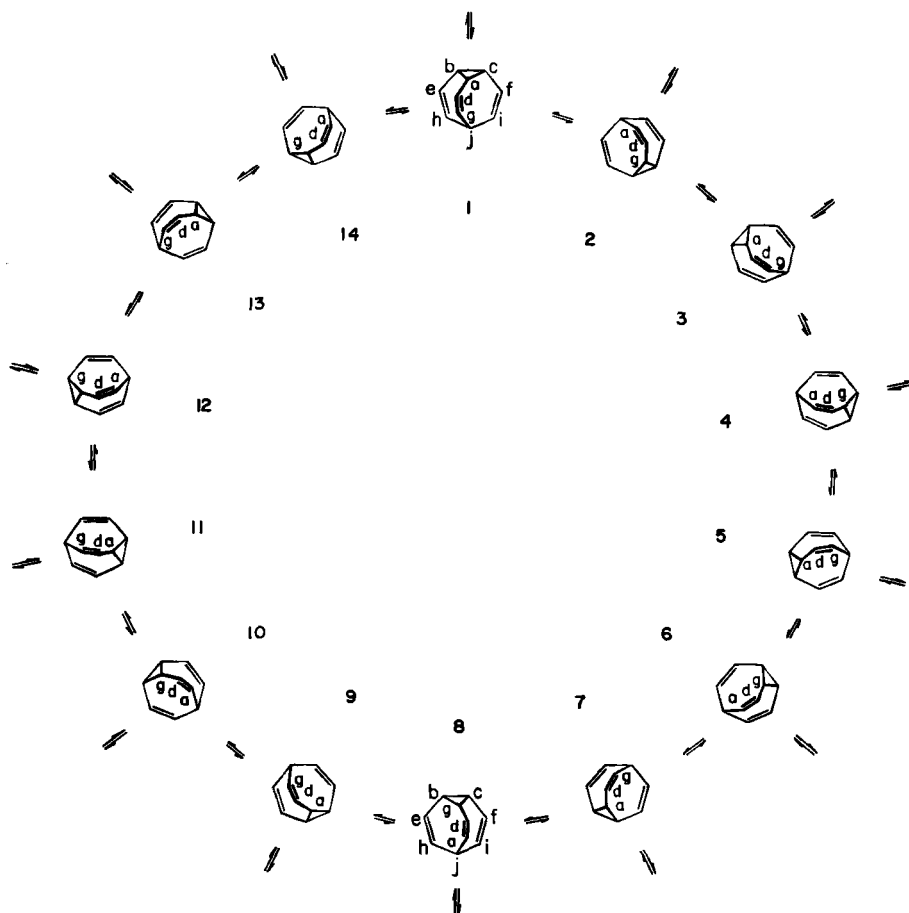[7]) See C. Berge, ibid., Chapter 2, for the definition of a planar graph.

Fig. 4. *A sequence of 14 isomerizations leaving the labelled molecule unchanged; the 14 structures implied form a cycle in the total graph.* Note that, after 7 isomerizations, the sequence of the ≡CH groups a, d, g is simply reversed

The graph has thus the structure illustrated by Figure 5.

2.3 The exchange diagram. No matter how complex the graph connecting the differently labelled structures, the exchange diagram, *i.e.* the diagram which shows how the nuclei exchange their sites, can be constructed considering one specifically labelled structure and the three directly connected ones (in doing so we recognize that the isomerization process in bullvalene can be treated as a *Markov* process). One then represents with arrows (one arrow per nucleus) how the different nuclei exchange between the different magnetic sites of the molecule. The nuclei are identified by letters (a, a, ..., j), the sites by numbers (1 to 4). In fact, due to the symmetry of the molecule, the exchange diagram can be obtained considering one specifically labelled structure and only one of the three directly connected ones. The exchange diagram of bullvalene is presented in Figure 6.
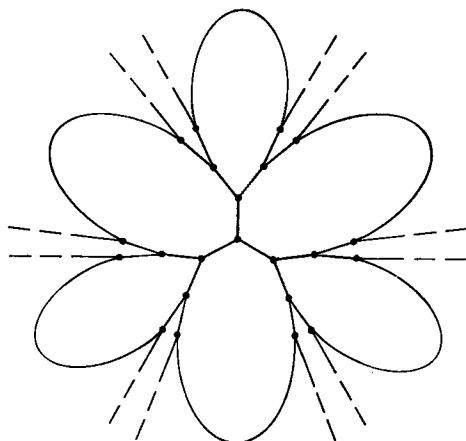
Fig. 5. *The structure of the graph representing the interrelations between all isomers*
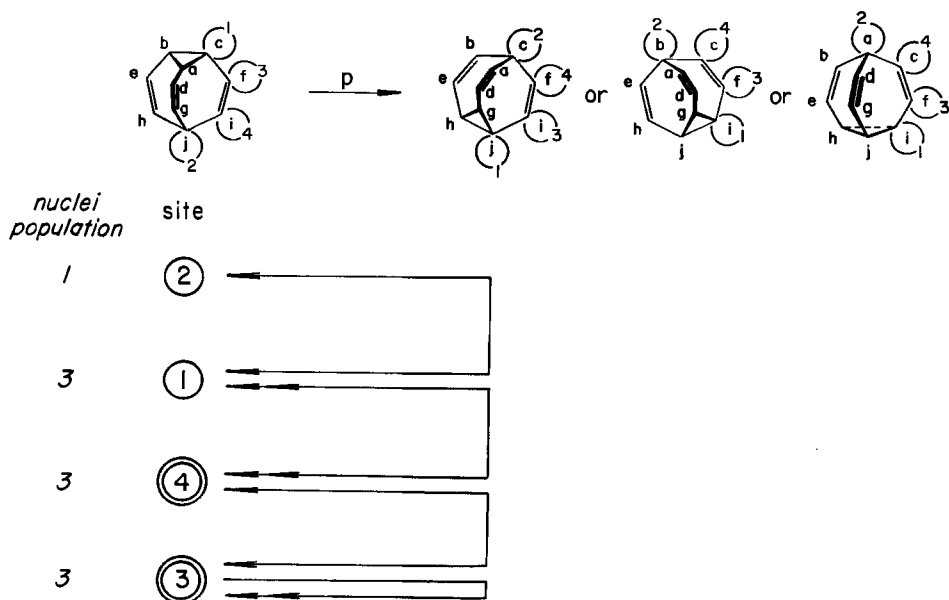

Fig. 6. *The exchange diagram for the Cope rearrangement in bullvalene*

One verification of the correctness of the exchange diagram lies in the fact that the total number of arrows arriving at one site must be equal to the nuclei population on this site. Note that the exchange diagram clearly indicates that, after several isomerization steps, any nucleus can occupy any site and thus that the spectrum in the fast exchange limit must consist of one single line.

3. Quantitative evaluation of the ¹H- and ¹³C- temperature dependent spectra of bullvalene. – 3.1. *Experimental details.* The ¹H- and ¹³C-NMR.-spectra of bullvalene have been obtained with a *Varian* XL-100-15″ spectrometer equipped with *Fourier* transform capabilities (16 K computer). Some modifications of the original V-4412 probe and of the temperature control

system have been made in order to improve the temperature constancy and to maintain it for long periods as required for the accumulation of the ^{13}C-free induction decays (24 h or more in some cases). The temperature was measured with a copper-constantan thermocouple located in an NMR. tube containing the same amount of solvent as the sample tube. The thermocouple junction was positioned in the tube at the height of the detection coil, while the reference junction was maintained at 0°. The temperature was measured before and after each measurement with the nitrogen gas flows used for the temperature control and for the spinning adjusted as during the experiments. The temperature could be maintained constant within $\pm 0.2°$ in all circumstances, even during the long-lasting ^{13}C-measurements.

The solutions used for the different measurements are listed in Table 1.

Table 1

Solution number	Nucleus observed	Temperature	Tube used[a])	Solvent	Bullv. mg	Solvent ml	Reference signal	Lock signal
1	^{1}H	– 115° to + 120°	sealed ampoule inside 5 mm tube	CS$_2$	12	0.4	TMS	^{1}H TMS
2	^{13}C	– 100° to + 40°	12 mm microcell	THF-d$_8$	60	2.5	TMS	^{2}H THF-d$_8$ high field s.
3	^{13}C	– 110° to – 20°	12 mm microcell	THF/CS$_2$ 1/4	60	2.5	TMS	^{2}H THF-d$_8$ high field s.
4	^{13}C	– 60° to + 20°	12 mm microcell	DMF-d$_7$	60	2.5	TMS	^{2}H DMF-d$_7$ carbonyl
5	^{13}C	+ 20° to + 150°	12 mm microcell	DMF-d$_7$	300	2.5	DMF-d$_7$ carbonyl	^{2}H DMF-d$_7$ carbonyl

[a]) All the tubes have been scaled.
  The 12 mm microcells used have been developed by us; they allow fast spinning without vortex formation.

The proton spectra have been recorded with a sweep width of 1000 Hz, and, when necessary, with sweep widths of 500, 250 and even 100 Hz. The sweep rate was always 1 Hz/s.

The ^{13}C-spectra (^{1}H-noise-decoupled) have been obtained in the *Fourier* transform mode. The free induction decays were accumulated with a spectral width of 5000 Hz. However, in the temperature domain corresponding to very slow or extremely fast exchange (relatively narrow lines) the spectral width was reduced to 2500 or 1000 Hz in order to have a sufficient number of points (channels) to characterize each peak. In the temperature domain where the signal is extremely broad (coalescence between olefinic and aliphatic carbon signals) some difficulties have been encountered: the number of free induction decays to be accumulated in order to obtain a reasonably good signal-to-noise ratio was so high that a spurious signal due to some cross-talk between the RF. transmitter and the detector was observed at the high field end of the spectrum (*i.e.* on the side of the carrier frequency). This very broad signal, out of phase with respect to the spectrum, could be substracted and did not affect the line shape analysis. For most of the spectra the ^{1}H-noise-modulated decoupling frequency was continuously on. At some temperatures, especially at those where only very slow exchange is observed, we have also used the gated ^{1}H-noise-decoupling mode in order to avoide *Overhauser* effects on the different signals. We have determined that when the different parameters such as acquisition time, pulse lenght, pulse delay ... are properly adjusted, the *Overhauser* effect is in fact the same for every line. This is to be expected since the bullvalene molecule has only $\equiv$CH groups. Typical ^{1}H- and ^{13}C-spectra are reproduced in Fig. 2 and 3.

3.2 *Assignment of the different signals in the spectra in absence of exchange.* – 3.2a *^1H-NMR. spectrum.* The assignment and the chemical shifts of the four ^1H-signals due to the four types of protons in the bullvalene molecule are indicated in Figure 2 (T = –60°). They result from ^1H-^1H-decoupling experiments as reported in Figure 7.
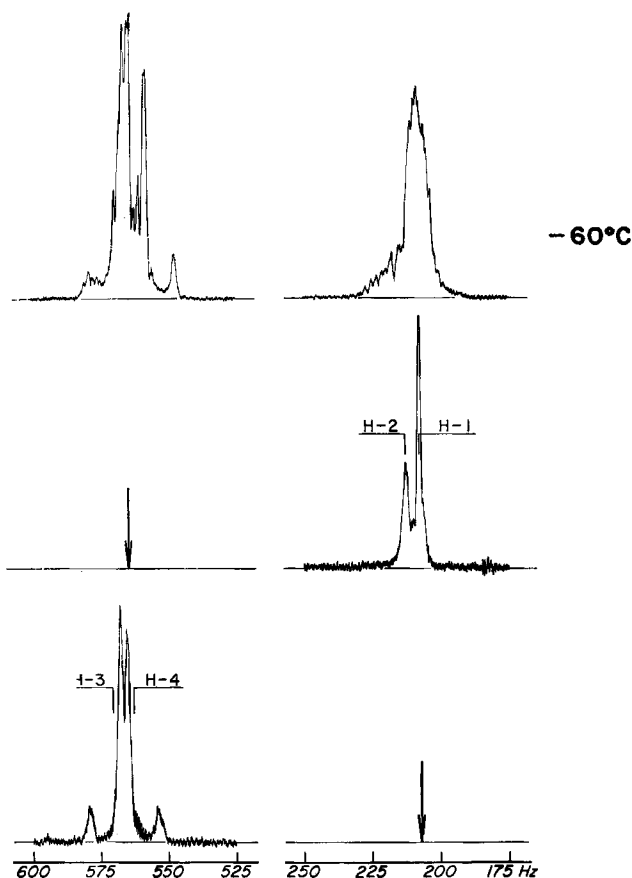

Fig. 7. *^1H—^1H-decoupling experiments performed at –60° in order to obtain the characteristic frequencies of the four magnetic sites*

3.2b *^{13}C-NMR. spectrum.* The assignment of the two ^{13}C signals in the aliphatic region is immediately deduced from their relative intensities. The assignment of the two equally intense signals due to the two types of olefinic carbons can be deduced from their relative broadening observed when the temperature is progressively increased (*vide infra*).

3.3 *Method of line shape calculation.* The line shape calculations have been performed using the *Anderson-Kubo-Sack* method, *i.e.* the expression:

$$I(\nu) = \mathbf{W} \; \text{Re} \; [2\pi i \, \mathbf{NU} + \pi\Delta - \mathbf{A}]^{-1} \, \mathbf{U}$$

in which:

W   is the population line vector characterizing the relative population on each site.

U   is the unity column vector.

NU is a diagonal matrix characterizing the frequency of the different sites.

Δ   is the relaxation matrix.

A   is the stochastic exchange matrix.

The population vector **W**. The elements w_i of this line vector express the relative nuclei population on site i. The sum of the elements is equal to unity

$$\sum_i w_i = 1 \, .$$

With the magnetic sites identified as indicated in Figure 6, we have

$$\mathbf{W} = [3/10, \ 1/10, \ 3/10, \ 3/10] \, .$$

The frequency matrix **NU**. The elements of this diagonal matrix are the characteristic frequencies ν_i of the magnetic sites i expressed in Hz and measured with respect to a given reference signal (TMS for both ^{1}H- and ^{13}C-spectra) in the usual way. When calculating the line shape, we have to take into account that the frequencies ν_i could be temperature dependent. For this reason we have measured the ^{1}H- and ^{13}C-spectra over a temperature range as great as possible in the slow exchange domain and we have deduced the corresponding temperature dependence of the chemical shifts. Furthermore, we have checked that the values of the resonance frequencies $\nu_i(T)$ extrapolated above coalescence are compatible with the frequency $\bar{\nu}$ of the fast exchange signal:

$$\nu = \sum_i w_i \, \nu_i(T)$$

For our line shape calculations we have adopted the following values (ν in Hz):

^{1}H (solution n° 1 in table 1; CS_2 + TMS)

$$\nu_1 = 211.46 - 0.02 \, T \, (°K) \qquad \nu_3 = 567.00 + 0.015 \, T$$
$$\nu_2 = 217.26 - 0.02 \, T \qquad\qquad \nu_4 = 552.71 + 0.045 \, T$$

^{13}C (solution n° 2 in table 1; THF-d_8 + TMS)

$$\nu_1 = 515.7 + 0.08 \, T \qquad\qquad \nu_3 = 3223.6 - 0.04 \, T$$
$$\nu_2 = 760.5 + 0.15 \, T \qquad\qquad \nu_4 = 3221.0 + 0.005 \, T$$

^{13}C (solution n° 3 in table 1; THF-d_8 + CS_2 + TMS)

$$\nu_1 = 510.1 + 0.08 \, T \qquad\qquad \nu_3 = 3195.9 + 0.02 \, T$$
$$\nu_2 = 744.4 + 0.15 \, T \qquad\qquad \nu_4 = 3200.8 + 0.02 \, T$$

^{13}C (solutions n° 4 and 5 in table 1; DMF-d_7)

$$\nu_1 = 528.4 \qquad\qquad\qquad\qquad \nu_3 = 3228.6$$
$$\nu_2 = 780.0 \qquad\qquad\qquad\qquad \nu_4 = 3232.9$$

ν (carbonyl C of solvent) $= 4123.6 - 0.065 \, T$

The relaxation matrix $\boldsymbol{\Delta}$. In principle the elements of this diagonal matrix are simply the line widths (in Hz) of the different resonance signals in absence of exchange. For calculating the ^{1}H-line-shape below coalescence, we have taken for Δ_{ii} the line-width of the multiplets as observed at low temperature. By doing this the contribution of ^{1}H-^{1}H-couplings to the line-shape is in some way taken into account. So we have used:

$$\Delta_{11} = \Delta \nu_1^0 = 9 \text{ Hz}, \quad \Delta_{22} = \Delta \nu_2^0 = 14 \text{ Hz}, \quad \Delta_{33} = \Delta \nu_3^0 = 6 \text{ Hz}, \quad \Delta_{44} = \Delta \nu_4^0 = 8 \text{ Hz}$$

For the fitting of the line-shape above coalescence and in the very fast exchange limit we have taken one unique value for the line-width, namely:

$$\Delta_{ii} = \Delta \nu_1^0 = \Delta \nu_2^0 = \Delta \nu_3^0 = \Delta \nu_4^0 = 0.2 \text{ Hz}$$

a value corresponding to the resolution that was achieved.

In the case of the ^{13}C-spectra, one unique value for the line-width was taken for all calculations:

$$\Delta_{ii} = \Delta \nu_1^0 = \Delta \nu_2^0 = \Delta \nu_3^0 = \Delta \nu_4^0 = 0.8 \text{ Hz}$$

This line-width was observed in slow exchange limit spectra taken with 5000 Hz or 1000 Hz as spectral width; it results from the digital filtering used for the *Fourier* transformation.

The stochastic exchange matrix **A**. The stochastic exchange matrix **A** entering the expression for the line shape as introduced by *Kubo-Tomita* can be shown to be identical with the **A** matrix of the *Kolmogorov* differential equations

$$\frac{d \, \mathbf{P}(t)}{dt} = \mathbf{P}(t) \, \mathbf{A} \qquad\qquad \frac{d \, \mathbf{P}(t)}{dt} = \mathbf{A} \, \mathbf{P}(t)$$

which express the time dependence of the transition probabilities

$$P(\Delta t) = P \, (j, t + \Delta t; \, i, t)$$

of a *Markov* process.

The off-diagonal elements of the **A** matrix are obtained as

$$a_{ij} = q_i \, Q_{ij}$$

where q_i (the intensity function in the terminology used for the theory of *Markov* processes) is simply the probability density p for a molecule to undergo one dynamic process; p is thus simply the rate of the isomerization in the true chemical sense. Q_{ij} are the relative probability functions; each Q_{ij} is obtained as the number of nuclei leaving the site i for site j divided by the number of nuclei occupying the site i (note that if more than one dynamic process are responsible for the exchange, the elements a_{ij} are obtained as

$$a_{ij} = \sum_k q_i^k \, Q_{ij}^k$$
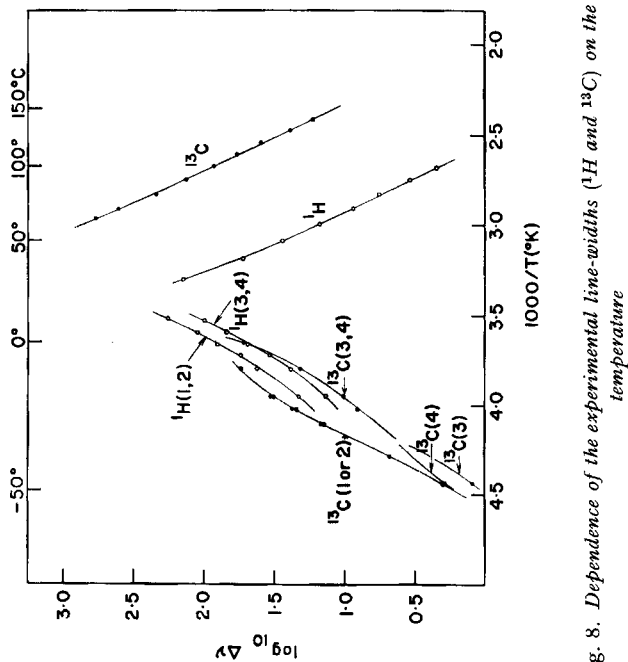
the summation being performed for all k).

90

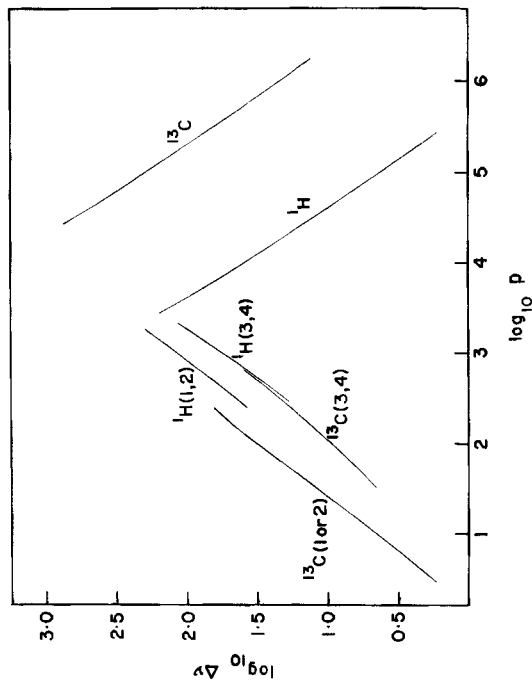Fig. 9. Dependence of the calculated line-widths (^1H and ^{13}C) on the isomerization rate

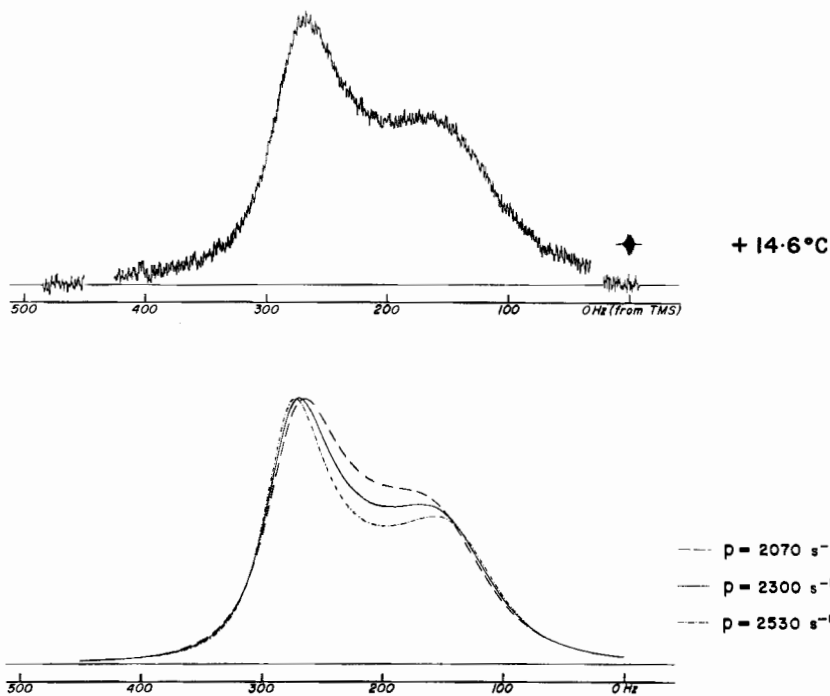Fig. 8. Dependence of the experimental line-widths (^1H and ^{13}C) on the temperature

Fig. 10. *¹H-spectrum of bullvalene observed at +14.6°* (coalescence of the olefinic and aliphatic signals) *and computed line-shape*
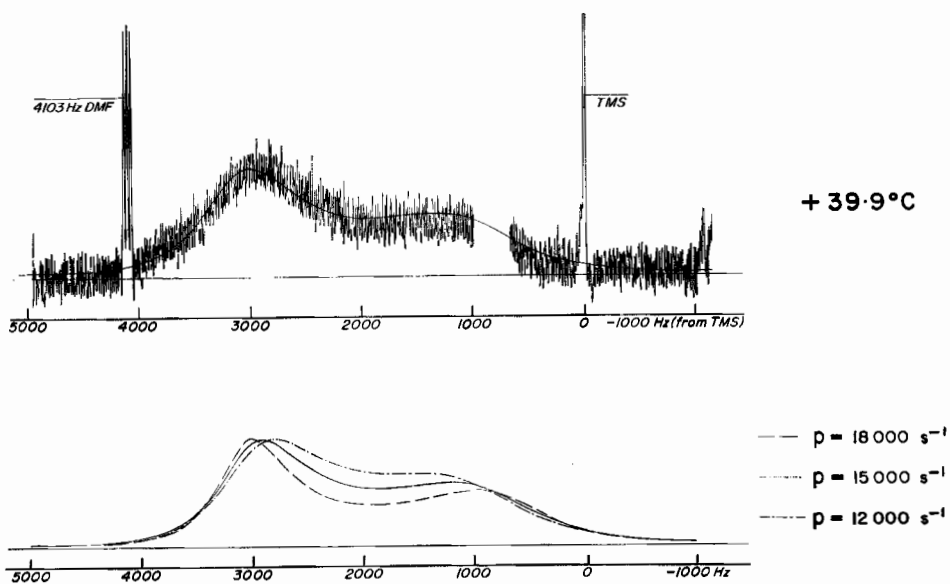

Fig. 11. *¹³C-spectrum of bullvalene observed at +39.9°* (close to coalescence of the olefinic and aliphatic signals) *and computed line-shape*

The diagonal elements of the matrix $\mathbf{A}$ are obtained as

$$a_{ii} = - \sum_{i \neq j} a_{ij} .$$

The matrix elements are readily deduced from the exchange diagram (Figure 6); one obtains:

$$\mathbf{A} = \begin{vmatrix} -p & p/3 & 0 & 2p/3 \\ p & -p & 0 & 0 \\ 0 & 0 & -p/3 & p/3 \\ 2p/3 & 0 & p/3 & -p \end{vmatrix}$$

3.4 *Results of the line-shape analysis.* The line-shapes of the ^{1}H- and ^{13}C-spectra have been computed according to the formalism mentioned above, using a computation program developed in 1964 and modified several times to increase its generality. The criteria used for the fitting were essentially the line-widths and, in some instances, the position and the relative intensity of extrema in the line-shape.

A first set of rate-temperature data was readily obtained by comparison of the experimental line-width/temperature relation with the calculated line-width/rate relation. Figure 8 shows how the experimental line-widths vary with temperature; Figure 9 shows that the calculated line-widths vary with the isomerization rate (log p) in an analogous manner. A first set of rate-temperature data was thus obtained by entering the line-width as single parameter in both graphs.

The kinetic parameters have then been refined by exact line shape fitting, taking into account the correct chemical shifts (*i.e.* the values extrapolated at each temperature) and line-widths. This exact line-shape fitting was especially required in the temperature domain where the olefinic and aliphatic signals coalesce into one single line. Figure 10 shows how the line-shape, in this temperature domain, is very sensitive to the value of p; in this figure we compare the ^{1}H-spectrum recorded at 14.5° with three calculated line-shapes, one corresponding to the exact fit (continuous line, p = 2300 s^{-1}), the other two corresponding to values of p respectively 10% smaller and 10% greater than the correct value. Figure 11 shows an analogous fit of one ^{13}C-spectrum.

The refined isomerization rates obtained gave the *Arrhenius* plot reproduced in Figure 12 and their regression led to the parameters reported in Table 2.

As can be seen from the table there is very good agreement between the kinetic parameters obtained from ^{1}H- and ^{13}C-data. In especially good agreement are the values of E_a and $\Delta H^{\neq}$, while the values of A, $\Delta S^{\neq}$, $\Delta G^{\neq}$ (0°) and k (0°) are slightly different. This corresponds to saying that the values of the rate p deduced from the ^{1}H-spectra are systematically smaller (by *ca.* 10%) than those deduced from the ^{13}C-spectra. This reflects the systematic error that can occur in one series of results (probably in the results deduced from the ^{1}H-spectra); the origin of such error is difficult to ascertain.

In Table 3 we have reported all the kinetic data available up to now concerning the *Cope* rearrangement of bullvalene. They all were obtained from ^{1}H-NMR. spectroscopy (coalescence temperatures at two radio frequencies, line-shape analysis,
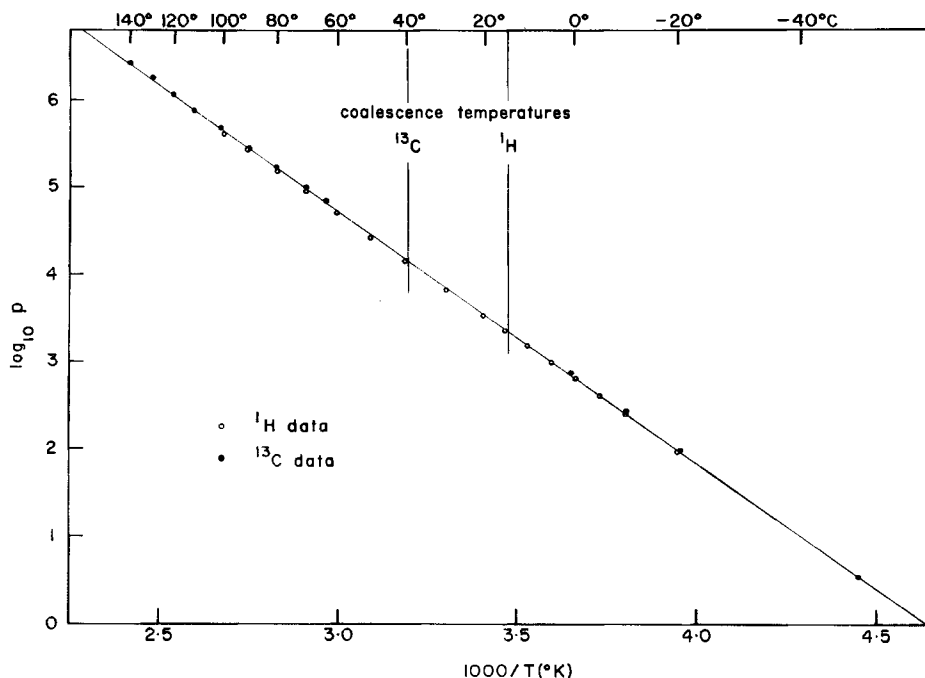
Fig. 12. *Arrhenius plot summarizing all the kinetic data (^1H and ^{13}C) obtained*

spin-echo measurements). It can be seen from this table that, although good correlation within each set of results was observed, systematic errors (in the experiments or/and in the quantitative interpretations) affect the data. This is particularly clear in the case of our previous line-shape analysis of the spectra recorded at 60 MHz. There we have a very good correlation within the data (30 values) and yet the E_a and $\Delta H^{\pm}$ values differ by as much as 1.5 kcal/mol from our new data. The origin of one systematic error affecting these old data lies in the fact that the line-widths in absence of exchange were not considered in our calculations ($\Delta_{ii} = 0$ for all i): the isomerization rates were thus overestimated at the high temperatures and underestimated at the low ones. An other source of systematic error has to be found in the technique used at that time (DP-60 *Varian* spectrometer without field-frequency lock, field sweep and not frequency sweep, scale calibration with audio side bands required for each spectrum). However, one can remark that the agreement between these old data and our new results is satisfactory.

4. Comparison of the ^1H- and ^{13}C-methods. – The good agreement between the data deduced from the 100 MHz ^1H- and the 25 MHz ^{13}C-measurements confirms our opinion that in the case of complex dynamic processes the line-shape analysis used here is precise and reliable. However, as pointed out above, the ^1H-spectra cannot always be quantitatively analysed while the ^{13}C-spectra can always be. In the case of bullvalene the analysis of the ^1H-spectra could be performed because the chemical shift difference between the exchanging signals (olefinic/aliphatic) is much

Table 2[a])

Nucleus observed	Number of obs.	Correlation factor	E_a kcal/mol	A 10^{13}	$k(0°)$ s^{-1}	$\Delta H^{\ddagger}$ kcal/mol	$\Delta S^{\ddagger}$ e.u.	$\Delta G^{\ddagger}(0°)$ kcal/mol
¹H (100 MHz)	15	0.99979	13.10 ± 0.08	1.96 ± 0.25	649 ± 15	12.56 ± 0.08	0.475 ± 0.25	12.43 ± 0.01
¹³C (25 MHz)	14	0.99994	13.13 ± 0.05	2.31 ± 0.15	727 ± 14	12.58 ± 0.05	0.798 ± 0.13	12.36 ± 0.01
¹³C+¹H	29	0.99969	13.18 ± 0.07	2.37 ± 0.25	671 ± 17	12.64 ± 0.07	0.848 ± 0.21	12.41 ± 0.01

[a]) The errors reported are the statistical errors.

Table 3[a])

Method	Ref.	Solvent	RF Freq. MHz	Temperature range °C	Number of obs.	Correlation factor	E_a kcal/mol	A 10^{12}	$k(0°)$ s^{-1}	$\Delta H^{\ddagger}$ kcal/mol	$\Delta S^{\ddagger}$ e.u.	$\Delta G^{\ddagger}(0°)$ kcal/mol
Coalescence at 2 frequencies [8])		CS₂	60 and 25	9.7° and −1.7°	2	–	12 ± 2					
Line-shape	[12]	.	60	10.5 to 80°	8	0.99969	11.64 ± 0.12	1.17 ± 0.22	569 ± 20	11.10 ± 0.12	−5.12 ± 0.37	12.50 ± 0.02
Line-shape	[13]	CS₂	60	−20° to 85°	30	0.99985	11.50 ± 0.10	1.28 ± 0.2	790 ± 15	10.9 ± 0.10	−4.8 ± 0.4	12.30 ± 0.02
Spin-echo	[14]	CCl₂=CCl₂	26.85	25° to 123°	12	0.99969	12.84 ± 0.10	777. ± 115	416 ± 16	12.3 ± 0.1	−1.37 ± 0.3	12.67 ± 0.02

[a]) The errors reported are the statistical errors based on regressions of the data as published.

[8]) J. F. M. Oth, Union Carbide European Research Associates, Technical Report, 1963. The value reported was obtained from the measurement of the coalescence temperatures at 60 MHz and 25 MHz, and calculated assuming that the rates are in the ratio 60/25.
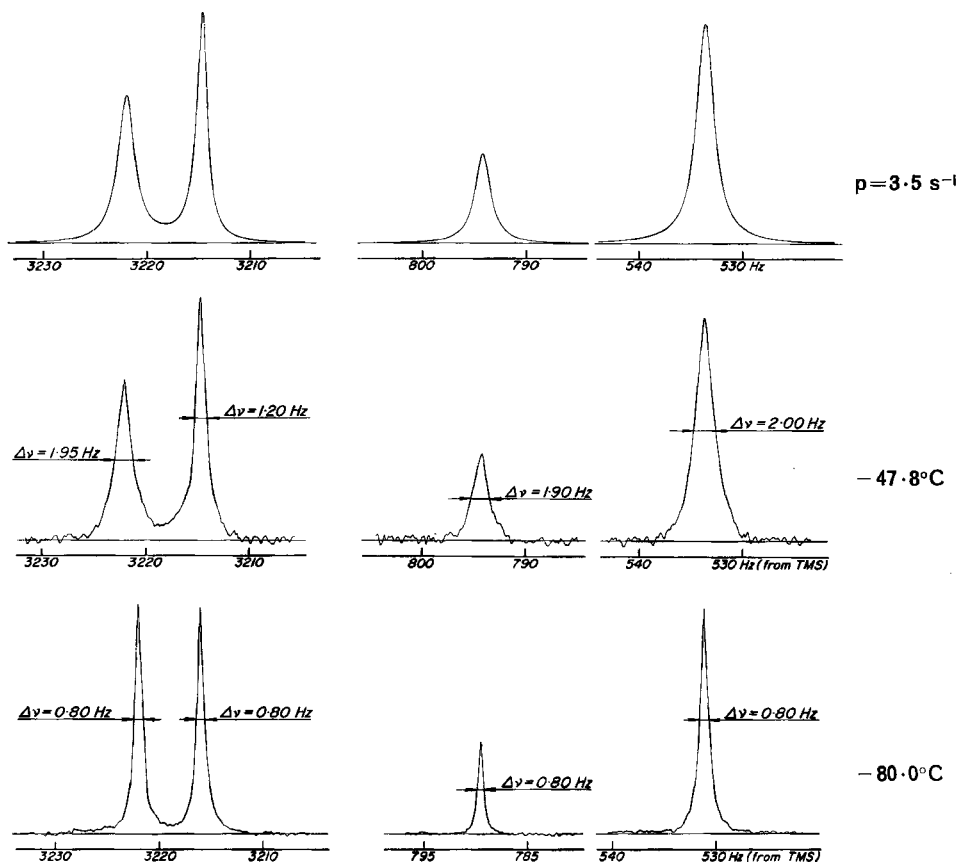
Fig. 13. *First broadening of the different ^{13}C-signals of bullvalene*

larger than the width of the multiplets observed for the protons on each site in the absence of exchange.

The potential advantage that ^{13}C-spectroscopy presents for the analysis of spectra of dynamic systems is clearly demonstrated when one considers the very first broadening of the lines. No valuable information can be deduced from the ^{1}H-spectra in this temperature domain, even for the case of bullvalene: the averaging of some coupling constants induces a very complex line-shape modification (overall narrowing of the olefinic and aliphatic signals is even observed when these signals collapse in a pseudo-singlet[9])). On the contrary, the ^{13}C-spectra contain much useful information concerning the mechanism responsible for the exchange. Figure 13 shows for instance the fitting of the ^{13}C-signals recorded at $-48.5°$; the isomerization rate is found to be 3.4 s^{-1}, a value consistent with all the others obtained. This implies that reliable kinetic data can be obtained even for very slow exchange. More specific information concerning the exchange mechanism can also be deduced from the very first broad-

[9]) This reminds us of the so-called 'exchange narrowing' some time observed in ESR. spectroscopy.

ening observed for each line. It can be shown that the broadening of the line charac-
teristic of site i is given by:

$$\Delta\Delta\nu_i = \Delta\nu_i - \Delta\nu_i^0 = \frac{1}{\pi}\sum_{i=j}a_{ij} = -\frac{a_{ii}}{\pi}$$

where $\Delta\nu_i$ is the line-width for the signal of the nuclei on site i, $\Delta\nu^0$ is the line-width
of the same signal in absence of exchange, a_{ii} is the corresponding diagonal element
of the matrix **A**.

This equation implies that it is possible to deduce the values of all the diagonal
elements of the matrix **A** from the first broadening observed, at a given temperature,
for each line of the ^{13}C-spectrum. At $-48.5°$ we have measured:

site 1	$\Delta\nu_1 = 2.00$ Hz	$\Delta\Delta\nu_1 = 1.20$ Hz	$-a_{11} = p = 3.77$ s^{-1}
site 2	$\Delta\nu_2 = 1.90$ Hz	$\Delta\Delta\nu_2 = 1.10$ Hz	$-a_{22} = p = 3.46$ s^{-1}
site 3	$\Delta\nu_3 = 1.20$ Hz	$\Delta\Delta\nu_3 = 0.40$ Hz	$-a_{33} = p/3 = 1.26$ s^{-1}
site 4	$\Delta\nu_4 = 1.95$ Hz	$\Delta\Delta\nu_4 = 1.15$ Hz	$-a_{44} = p = 3.61$ s^{-1}
			$\langle p = 3.65$ s$^{-1}\rangle$

The line-width in absence of exchange was taken as 0.8 Hz, the value observed
at $-80°$ under the same experimental conditions (spectrum width 500 Hz, same digital
exponential filter). Thus it is indeed possible to confirm from the first broadening of
each ^{13}C-line that the value of the matrix element a_{33} is 1/3 that of any of the other
three elements $a_{11} = a_{22} = a_{44}$. This is a direct information concerning the exchange
mechanism which cannot be obtained from the ^1H-spectra.

It is worth noting here that if measurements of transfer of spin-polarization between
the different lines of the ^1H-noise-decoupled ^{13}C-spectrum could be performed in the
FT mode (this is in principle possible: it requires a second oscillator of 25 MHz with
adjustable offset frequency and an adequate gating circuitry[10]), it would be possible
to deduce the relative values of all the elements a_{ij} (i = j and i ≠ j) of the matrix **A**.
Complete information concerning the exchange mechanism (*i.e.* all Q_{ij} values) would
then be obtained. It is clear that this experimental approach would be extremely
valuable in the investigation of molecules for which the processes responsible for the
exchange are not so evident as the *Cope* rearrangement in bullvalene.

Note added in proof: A ^{13}C-NMR. investigation of the dynamic behaviour of bullvalene has
meanwhile appeared in the literature (*H. Nakanishi & O. Yamamoto*, Tetrahedron Letters *20*,
1803 (1974)). The kinetic parameters reported therein differ appreciably from ours and from the
previous ones cited in the literature (see Tables 2 and 3 above).

REFERENCES

[1] *H. S. Gutowsky & C. H. Holm*, J. Chem. Phys., *25*, 1228 (1956).
[2] *P. W. Anderson*, J. Phys. Soc. Japan, *9*, 316 (1954).
[3] *R. Kubo & K. Tomita*, J. Phys. Soc. Japan, *9*, 888 (1954).

[10] We plan to develop this technique using our XL-100 spectrometer and a frequency synthesizer.

[4] *R. A. Sack*, Mol. Phys., *1*, 163 (1958).

[5] *S. Alexander*, J. Chem. Phys., *37*, 967 (1962).

[6] *J. M. Delpuech*, Mol. Phys., *14*, 567 (1968).

[7] *G. Binsch*, Mol. Phys., *15*, 469 (1968).

[8] *J. F. M. Oth & J.-M. Gilles*, Tetrahedron Letters, *1968*, 6259; *J.-M. Gilles, J. F. M. Oth, F. Sondheimer & E. P. Woo*, J. Chem. Soc. B *1971*, 2177; *J. F. M. Oth*, Pure and Applied Chemistry, *25*, 573 (1971).

[9] *W. E. von Doering & W. R. Roth*, Angew. Chem., *75*, 27 (1963); Tetrahedron *19*, 715 (1963).

[10] *G. Schröder*, Chem. Ber., *97*, 3140 (1964); *R. Merényi, J. F. M. Oth & G. Schröder*, Chem. Ber., *97*, 3150 (1964).

[11] *M. Saunders*, Tetrahedron Letters *1963*, 1699.

[12] *J.-M. Gilles*, Thèse de doctorat (Physique), Université Libre de Bruxelles, 1969. These results have been reported at the 8th European Congress on Molecular Spectroscopy, Communication No. 389, Copenhagen 1965, by J.-M. Gilles and J. F. M. Oth.

[13] *A. Allerhand & H. S. Gutowsky*, J. Amer. chem. Soc., *87*, 4092 (1965).

---

157. Action du chlorure de nitrosyle sur le trichloréthylène et sur le tétrachloréthylène

par **Yves Calvez**[1]), **Jacques Tuaillon**[2]) et **Roger Perrot**[2])

(21. II. 74)

Summary. Nitrosyl chloride is only chlorinating in darkness and above 100°. In the sun light and at room temperature it reacts as a chlorinating, nitrosating, nitrating and oxidizing agent. With trichlorethylene in fact pentachlorethane 1,1,1,2-tetrachloro-2-nitrosoethane, 1,1,1,2-tetrachloro-2-nitroethane, dichloracetic acid and a compound of empirical formula $C_4H_2Cl_5NO_2$ are obtained. Tetrachloroethylene carried to hexachlorethane, pentachloronitrosoethane and tetrachloro-2-(pentachlorethyl)-1,2-oxazetidine.

Introduced nitrosyl chloride provided nitrogen monoxide prouved by gaz chromatography. This monoxide reacted afterwards to give nitrogen which is the single nitrogenous gazeous compound. Carbondioxide is a minor component of the gaz.

L'étude de l'action du chlorure de nitrosyle sur les dérivés halogénés de l'éthylène fait l'objet des travaux de *Haszeldine* [1] [2], de *Yakoubovitch* [3] et de *Lacher* [4].

Yakoubovitch fait réagir NOCl sur $CH_2=CHCl$, $CH_2=CCl_2$, $CCl_2=CHCl$, $CH_2=CHF$, $CHF=CHCl$, $CF_2=CHCl$, $CCl_2=CHF$ et $CF_2=CFCl$. Ces réactions qui ont lieu en tubes scellés et à la température ordinaire permettent d'obtenir des dérivés chlorés ou chloronitrés.

Haszeldine fait réagir le chlorure de nitrosyle dans des conditions opératoires différentes. A 100 °C et en tube scellé il obtient des composés dichlorés et chloronitrés avec $CF_2=CF_2$, $CF_2=CFCl$, $CF_2=CCl_2$ et $CHCl=CCl_2$. Il note l'analogie des composés obtenus avec ceux de *Yakoubovitch*.

Lacher fait réagir NOCl sur $CF_2=CF_2$ en présence de $FeCl_3$ anhydre à 45 °C et obtient essentiellement les composés nitrosochlorés correspondants à côté de com-

[1])   Société d'Electro-chimie, d'Electro-métallurgie et des Aciéries électriques d'Ugine, Paris.

[2])   Laboratoire de Chimie Générale, Faculté des Sciences, 32 rue Mégevand, 25030 Besançon Cedex.